Wargenau *et al. Biointerphases* 2013, **8**:7
http://www.biointerphases.com/content/8/1/7

Biointerphases
a SpringerOpen Journal

ORIGINAL ARTICLE Open Access

Linking aggregation of *Aspergillus niger* spores to surface electrostatics: a theoretical approach

Andreas Wargenau*, Ingo Kampen and Arno Kwade

Abstract

The effect of medium pH on conidial aggregation during submerged cultivation of *Aspergillus niger* is considered to originate from the electrostatic surface properties of the spores. As previously shown, these properties are greatly influenced by the presence of a melanin-containing surface coating covering the outer spore wall layer. The present study was designed to elucidate the impact of such a coating on the spores' surface potential and their electrostatic repulsion under acidic conditions. A Poisson–Boltzmann model was proposed and potential profiles across the surface coating of noninteracting and interacting spores were calculated. The surface potentials thus obtained were in line with the observed pH dependence of the zeta potential. This dependence was consistent with the outcome of aggregation experiments. Apparently contradictory results regarding the zeta potential and the aggregation behavior of the spores were obtained when the ionic strength was varied. However, both of these observations could be explained by the model.

Keywords: *Aspergillus niger*, Melanin, Surface potential, Electrostatic interaction, Aggregation

Background

Forces originating from the electric surface charge of fungal spores are generally suspected to play a key role in both spore–surface [1-4] and spore–spore [4-6] attraction. Characterization of these forces is, hence, of great interest, especially in consideration of biofilm formation [7] and spore aggregation during submerged cultivation [8]. Unfortunately, little is known about the electrostatics of fungal spore surfaces. In the case of the biotechnological workhorse *Aspergillus niger*, the tendency to form conidial aggregates at the early stage of cultivation has long been recognized [9] and aggregation behavior was attributed to electrostatic surface properties [10-12]. However, there is presently no uniform explanation linking the pH dependence of these properties to that of the aggregation behavior during cultivation.

A common approach to assess the charge properties of microbial cells is to experimentally determine their electrophoretic mobility or zeta potential. In the case of hard particles, where fixed charges are assumed to be located in a plane, the zeta potential can be used to predict aggregation behavior on the basis of conventional DLVO theory. In contrast, in models of biological cells, it is typically assumed that fixed charges are distributed throughout an ion-penetrable surface layer of finite thickness [13-16]. This has two prominent consequences from a theoretical point of view. On the one hand, the attribution of the cells' electrophoretic mobility or zeta potential to a single potential value with distinct physical meaning, like the surface potential, is valid only under certain circumstances [17]. On the other hand, electrostatic repulsion between the cells can no longer be predicted from the zeta or surface potential alone [18].

In a previous study, we investigated the origin of the electric surface charge of *A. niger* spores under acidic conditions [19]. In these investigations, the typical electrophoretic behavior of the spores, which is characterized by negative mobilities over a wide range of pH values [10,12,20], was traced to the presence of melanin pigments. These pigments were found to be located in a distinct layer on top of the outer spore wall layer, where they contribute to the net surface charge by partial dissociation of melanin-bound carboxyl groups.

*Correspondence: wargenau@a-wargenau.de
Institut für Partikeltechnik, Technische Universität Braunschweig, Volkmaroder Straße 5, 38104 Braunschweig, Germany

In the present study, we examined the electrostatic effect of such a melanin-containing surface coating on the surface potential and aggregation behavior of the spores in acidic environments. We used Poisson–Boltzmann mean-field theory [21] to calculate the potential profiles across the spore–solution and spore–spore interfaces of noninteracting and interacting spores and compared the theoretical outcomes with data from electrophoretic measurements and aggregation experiments.

Theory

Electrostatic surface model

An electrostatic model of the spore surface was built in accordance with our previous findings [19]. The model consists of a planar plate covered by an ion-penetrable coating of thickness δ. The coating contains uniformly distributed fixed ionizable groups at density $|\rho_{\mathrm{fix},0}/e|$, where e is the elementary charge and $\rho_{\mathrm{fix},0}$ denotes the space charge density at complete dissociation. Additionally, a constant surface charge density σ is considered at the inner boundary of the coating to allow for an electric field contribution from the spore wall.

Poisson–Boltzmann model

Consider two similar parallel spore surfaces immersed in a symmetrical electrolyte and separated at a distance $d - 2\delta$, as indicated in Figure 1. Taking the z axis as perpendicular to the surfaces and choosing $z = 0$ at the outer spore wall boundary of one spore surface, we can express the electric potential between the spore walls through the following Poisson equations:

$$\frac{d^2\Psi(z)}{dz^2} = -\frac{1}{\epsilon_0\epsilon_\mathrm{r}}\left[\,\rho_+(z) + \rho_-(z) + \alpha(z)\rho_{\mathrm{fix},0}\,\right] \quad \text{for} \quad 0 < z < \delta, \tag{1}$$

$$\frac{d^2\Psi(z)}{dz^2} = -\frac{1}{\epsilon_0\epsilon_\mathrm{r}}\left[\,\rho_+(z) + \rho_-(z)\,\right] \quad \text{for} \quad \delta < z < d/2. \tag{2}$$

In these equations, $\rho_+(z)$ and $\rho_-(z)$ describe the z-dependent space charge densities of positive and negative mobile ions, $\alpha(z)$ is the position-dependent degree of dissociation of the fixed ionizable groups (here carboxyl groups), ϵ_0 denotes the permittivity of free space, and ϵ_r denotes the relative permittivity of the solution and surface coating. Note that, for reasons of symmetry ($\Psi(z) = \Psi(d - z)$), only half of the region between the outer spore wall layers is regarded.

If we define the electric potential to be zero in the bulk solution (e.g., at $z = d/2$ for $d - 2\delta \to \infty$) and assume that mobile charges obey a Boltzmann distribution, we may express their respective charge densities by

$$\rho_+(z) = +|\nu| b_+(z) e N_\mathrm{A} C_\mathrm{I}^\infty \mathrm{e}^{-\frac{|\nu| e\Psi(z)}{kT}}, \tag{3}$$

$$\rho_-(z) = -|\nu| b_-(z) e N_\mathrm{A} C_\mathrm{I}^\infty \mathrm{e}^{+\frac{|\nu| e\Psi(z)}{kT}}, \tag{4}$$

where N_A denotes the Avogadro constant; k, the Boltzmann constant; T, the temperature; $|\nu|$, the absolute value of the ion's valence; and C_I^∞, the molar concentration of cations and anions in the bulk solution. $b_+(z)$ and $b_-(z)$ are dimensionless functions taking values between

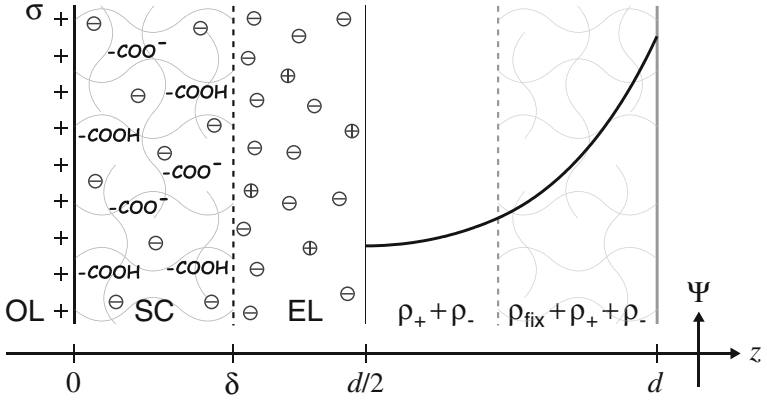

Figure 1 Schematic representation of the Poisson–Boltzmann model for the investigation of the potential distribution across the spore–solution or spore–spore interface of noninteracting and interacting *A. niger* spores. The electric potential is considered to arise from three different charge contributions: (i) a surface charge density σ at the outer boundary of the outer spore wall layer (OL), (ii) the nonuniform space charge density of ionized fixed carboxyl groups in the surface coating (SC), ρ_{fix}, and (iii) the space charge densities ρ_+ and ρ_-, covering the charge contributions from mobile positive and negative ions in the electrolyte solution (EL) and in the ion-penetrable surface coating.

0 and 1 for $0 < z < \delta$ and equal unity for $\delta < z < d/2$. Physically, these functions can be viewed as intrinsic position-dependent partition coefficients describing local diminished ion solubilities in the surface coating [22].

The contribution from fixed charges in the surface coating may also be expressed as a function of the electric potential [21]. Combining the law of mass action of the corresponding dissociation equilibrium with the Boltzmann distribution for hydronium ions leads to

$$\alpha(z) = \frac{1}{\frac{C^{\infty}_{H_3O^+}}{K_a} e^{-\frac{e\Psi(z)}{kT}} + 1}, \tag{5}$$

where K_a is the equilibrium constant of the dissociation reaction and $C^{\infty}_{H_3O^+}$ is the bulk concentration of hydronium ions.

Substituting equations 3, 4, and 5 into equation 1 and equations 3 and 4 into equation 2 finally yields the Poisson–Boltzmann equations of the model system:

$$\begin{aligned}\frac{d^2\Psi(z)}{dz^2} = &-\frac{1}{\epsilon_0\epsilon_r}|\nu| e N_A C_I^{\infty} \\ &\times \left(b_+(z) e^{-\frac{|\nu| e\Psi(z)}{kT}} - b_-(z) e^{+\frac{|\nu| e\Psi(z)}{kT}} \right) \\ &- \frac{1}{\epsilon_0\epsilon_r} \frac{\rho_{fix,0}}{\frac{C^{\infty}_{H_3O^+}}{K_a} e^{-\frac{e\Psi(z)}{kT}} + 1} \quad \text{for} \quad 0 < z < \delta,\end{aligned} \tag{6}$$

$$\frac{d^2\Psi(z)}{dz^2} = \frac{2}{\epsilon_0\epsilon_r}|\nu| e N_A C_I^{\infty} \sinh\left(\frac{|\nu| e\Psi(z)}{kT}\right) \quad \text{for} \quad \delta < z < d/2. \tag{7}$$

Boundary conditions result from continuity in the electric potential and the electric field at $z = \delta$, that is,

$$\Psi(z \to \delta^-) = \Psi(z \to \delta^+), \tag{8}$$

$$\left.\frac{d\Psi(z)}{dz}\right|_{z\to\delta^-} = \left.\frac{d\Psi(z)}{dz}\right|_{z\to\delta^+}, \tag{9}$$

as well as from electroneutrality, which implies

$$\left.\frac{d\Psi(z)}{dz}\right|_{z=d/2} = 0, \tag{10}$$

$$\left.\frac{d\Psi(z)}{dz}\right|_{z=0} = -\frac{\sigma}{\epsilon_0\epsilon_r}. \tag{11}$$

The latter condition stems from the requirement that the electric field at $z = 0$ is twice the electric field arising from the spore wall. This requirement together with the other boundary conditions and the differential equations 6 and 7 determines the desired potential distribution.

Interacting vs. noninteracting case

The Poisson–Boltzmann model described above provides solutions not only for the case of an interacting spore surface but also for the case of a noninteracting spore surface. Those are obtained for $d - 2\delta \to \infty$.

For an interacting surface, we will further distinguish between the case where the surface is in direct contact with its counterpart, meaning $d - 2\delta = 0$, and the case where the surfaces are separated at a distance $d - 2\delta > 0$. In the former, depending on the balance between all interfacial forces, the surface coating may be compressed. To account for this possibility, we introduce the quantities $\rho^*_{fix,0}$ and δ^*, which, respectively, represent the space charge density of fixed charges at complete dissociation and the thickness for the uncompressed surface coating. Furthermore, we assume that the uniform density of the fixed ionizable groups increases proportionally to the ratio of compression. The actual charge density of fixed charges at complete dissociation is then given by

$$\rho_{fix,0} = \rho^*_{fix,0}\frac{\delta^*}{\delta}. \tag{12}$$

Methods

Microorganism, cultivation, and preparation of spore suspensions

Spores of *Aspergillus niger* AB1.13 [23] were kindly provided by P. J. Lin and R. Krull (Institute of Biochemical Engineering, Technische Universität Braunschweig, Germany). The cultivation on agar plates, the harvesting, and the determination of the spore concentration of final suspensions were carried out in the same manner as that described in Lin et al. [24], except that the plates were incubated for 4 days.

For the purpose of electrophoretic measurements and aggregation experiments, the spores were centrifuged and resuspended in different aqueous solutions by ultrasonication. The solutions contained either a mixture of NaCl and HCl (pH 2–3.5) or NaCl only (pH 5, determined by comparison with buffered suspensions of known pH using methyl red as an indicator). Sonication was performed with a Labsonic L sonicator (B. Braun, Melsungen, Germany) at 0.2 W mL^{-1} for 20 min with stirring and cooling with ice water.

Zeta potential determination

Suspensions with a spore concentration of 10^6 mL^{-1} were used for measuring electrophoretic spore mobility by means of a Zeta Master S (Malvern Instruments, Malvern, UK). Zeta potentials were calculated by the Smoluchowski equation [25] from the mean of 4–5 measurements.

Aggregation experiments

Spore aggregation was assessed in a baffled blade-stirred vessel, designed in accordance with the dimensions given

in Zlokarnik and Judat [26]. Spore suspensions with a volume of 500 mL and a spore concentration of 5×10^6 mL^{-1} were stirred at 500 rpm (corresponding to a volumetric power input of approximately 1.8 kW m^{-3}) and ambient temperature. Samples were taken at different time intervals using an inoculation loop, transferred to glass slides, and photographed under an inverted microscope after the settling of the spores.

To evaluate the degree of aggregation at steady-state conditions, photographs of samples obtained after 80, 100, and 120 min of stirring were analyzed. The number of isolated spores, N_1; and the number of aggregates consisting of two spores, N_2; three spores, N_3; and four spores, N_4, were counted within a uniform area containing a total of at least 500 spores. The number of spore pairs built during settling, N_2^s, was estimated for the purpose of correcting the counted number of pairs using the assumption that $2N_2^s \approx N_1^0 - N_1 \approx PN_1^0(N_1^0 - 1)$. Here, N_1^0 denotes the number of single spores before settling and P is the probability that the centers of two single spores within the analyzed area were at distance $r < 4.6$ μm, which was the criterion applied to define aggregates during counting. The fraction of spores present in the aggregates at each time point was then estimated by using

$$\frac{N_{ag}}{N_{tot}} \approx \frac{2N_2 - 2N_2^s + 3N_3 + 4N_4}{N_1 + 2N_2 + 3N_3 + 4N_4}. \quad (13)$$

Determination of potential distributions

To obtain potential distributions that satisfy equations 6 to 11, a numerical approach was followed. With this approach, the equations were not solved directly, but rather solutions were obtained by solving the concentration profiles of mobile ions. A detailed description thereof can be found in the electronic supplementary material (see Additional file 1).

All calculations were performed for T = 298.15 K, ϵ_r = 78.4, $|\nu|$ = 1, $\rho^*_{fix,0} = -10^8$ C m^{-3}, and $K_a = 10^{-4.3}$ mol L^{-1} (note that the two latter quantities were estimated from the results of titration and extraction experiments [19]). $b_+(z)$ and $b_-(z)$ were chosen to equal unity for all values of z unless stated otherwise.

Results

Zeta potential

The electrophoretic mobilities of spores were determined in aqueous solutions of different pH and NaCl concentrations. The corresponding zeta potentials as calculated by the Smoluchowski equation are given in Figure 2. All values observed were negative and decreased with increasing pH. By considering the dependence on the ionic strength at constant pH, a clear trend of decreasing potentials with decreasing NaCl concentration was seen for the two lower pH values. Although the same trend was basically true for pH 3, the reduction of the NaCl concentration from 0.05 to 0.01 mol L^{-1} led to comparatively little change in the potential. At pH 2.5, even a small increase in the zeta potential was noted for the same reduction in NaCl concentration, resulting in a minimum zeta potential value at 0.05 mol L^{-1}.

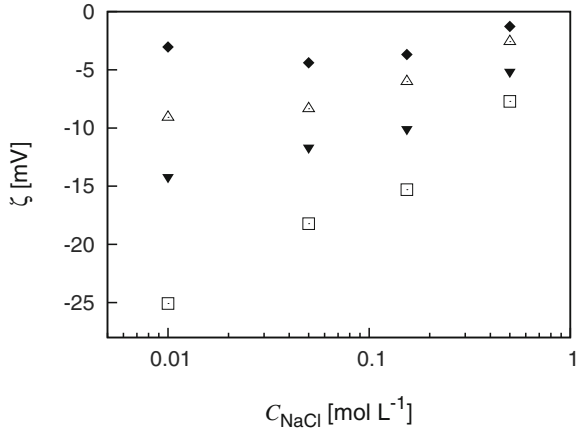

Figure 2 Electrophoretic behavior of *A. niger* spores. Shown is the zeta potential as a function of NaCl concentration, determined at pH 2.5 (◆), pH 3 (△), pH 3.5 (▼), and pH 5 (□).

Spore aggregation

To assess the impact of the electrostatic surface properties of the spores on their aggregation behavior, the aggregation tendencies at different pH values were studied in a turbulent stirred vessel. The amount of spores present in the aggregates at steady state was found to be highest at pH 2.5 and lowest at pH 5, as can be seen from Figure 3a. At pH 5, no or very little aggregation occurred, as indicated by the slightly negative ratio of aggregated spores (note that negative values of N_{ag}/N_{tot} may occur in the case of low aggregation because of uncertainties in the statistical correction for misclassification of spore pairs). This tendency is generally in line with expectations from obtained zeta potential values. However, aggregation behavior observed for varying NaCl concentrations at pH 2.5 (Figure 3b) indicated a more complex relation to corresponding electrokinetic data. The estimated ratio of aggregated spores increased by a factor of ~3 when the NaCl concentration was increased from 0.01 to 0.154 mol L^{-1} and again decreased by a similar factor when the NaCl concentration was further increased to 0.5 mol L^{-1}.

Influence of the pH Value on the potential distribution at noninteracting spore surfaces

In the present model, we have considered the effect of bulk pH on the z-dependent degree of ionization in the surface coating. Additionally, a variable surface charge density has been introduced to account for a pH-dependent charge

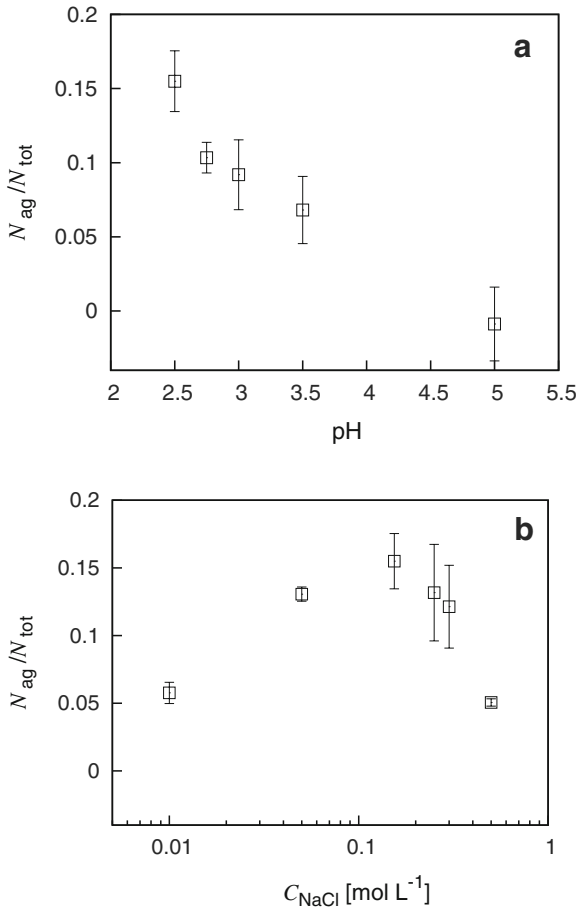

Figure 3 Spore aggregation in stirred suspensions of different pH and NaCl concentrations. Diagrams show means and standard deviations (error bars) of estimated relative amounts of spores present in aggregates after 80, 100, and 120 min of stirring (steady state). The pH-dependent data (**a**) refer to a NaCl concentration of 0.154 mol L^{-1} and the data determined as a function of salt concentration (**b**) refer to a pH of 2.5.

contribution from the spore wall. However, as discussed in our previous paper [19], the thickness of the surface coating may also change with the solution pH. This assumption is based on the observation that partial ionization of melanin-associated carboxyl groups is accompanied by an irreversible release of melanin pigments.

Figure 4 elucidates the impact of the thickness of the surface coating on the potential distribution at the spore surface. In principle, two general cases can be distinguished: 1. In the "thin coating" case, the surface potential ($\Psi(z = \delta)$) depends on the charge contribution of the spore wall as well as on the thickness of the surface coating. 2. In the "thick coating" case, we assume the coating to be large enough that, owing to the shielding effect of counterions, the electric field vanishes almost completely far inside. In this instance, the surface potential will be more or less independent of the charge contribution from

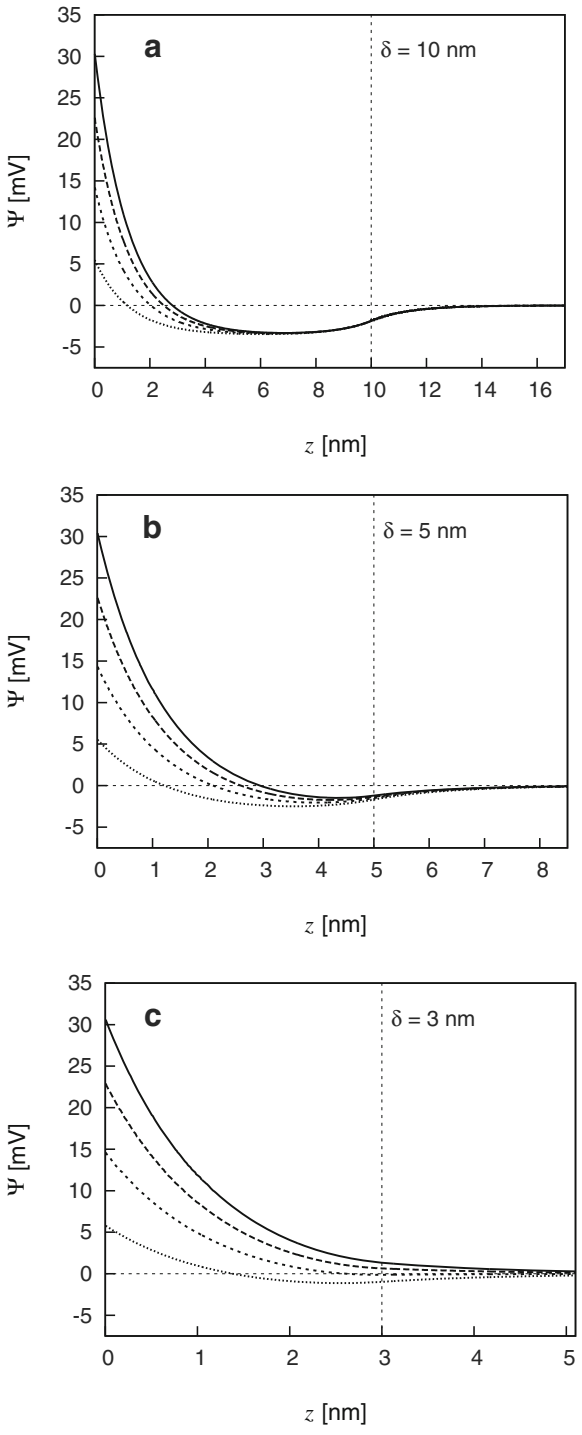

Figure 4 Influence of the thickness of the surface coating on the electric potential distribution at low bulk pH. Each diagram shows potential profiles as determined for several different electric field contributions of the spore wall. Calculation conditions are as follows: σ = 0.02 C m^{-2} (——), 0.015 C m^{-2} (– – –), 0.01 C m^{-2} (– – –), 0.005 C m^{-2} (.....); δ = 10 nm (**a**), 5 nm (**b**), 3 nm (**c**); $C^{\infty}_{H_3O^+} = 10^{-2.5}$ mol L^{-1}; $C^{\infty}_{I} = 0.05$ mol L^{-1}.

the spore wall and also of the actual thickness of the coating.

An example for a thick coating is given in Figure 4a. Under the chosen bulk solution conditions (C_{I}^{∞} = 0.05 mol L^{-1}, $C_{H_3O^+}^{\infty} = 10^{-2.5}$ mol L^{-1}) a value of δ of 10 nm is large enough that an effective surface charge density in the range of 0.005 to 0.02 C m^{-2} has virtually no effect on the surface potential. Moreover, in agreement with the aforementioned, the minimum potentials inside the coating, ranging from -3.31 to -3.45 mV, lie close to the potential of completely vanishing electric field. This theoretical value, which we will further denote as the layer potential Ψ_{l}, is determined to be -3.61 mV by the following electroneutrality expression [21]:

$$-2eN_{\mathrm{A}}C_{\mathrm{I}}^{\infty}\sinh\left(\frac{e\Psi_{\mathrm{l}}}{kT}\right)+\frac{\rho_{\mathrm{fix}}^{0}}{\frac{C_{H_3O^+}^{\infty}}{K_{\mathrm{a}}}\mathrm{e}^{-\frac{e\Psi_{\mathrm{l}}}{kT}}+1}=0. \qquad (14)$$

Solutions obtained for δ = 5 nm and δ = 3 nm under otherwise identical conditions, in contrast, show a significant dependence on the surface charge density (Figure 4b and c). Particularly, the profiles determined for δ = 3 nm make it clear that with a thin coating positive surface potentials can occur at low bulk pH values owing to a positive charge contribution from the spore wall.

The direct influence of the bulk pH on the electric potential across the spore–solution interface was investigated for δ = 5 nm and σ = 0 (where again C_{I}^{∞} was chosen to be 0.05 mol L^{-1}). Solutions obtained in such a way can be viewed as general interfacial electric potential profiles of a thick coating. This is because the potential values achieved for z = 0 are very close to the theoretical layer potential ($\Psi(z=0)-\Psi_{\mathrm{l}} < 0.1$ mV) and, hence, approximately reflect the boundary conditions of respective infinite-thick coatings.

The solutions, which are depicted in Figure 5 (solid curves), indicate the expected qualitative dependence of the surface potential on the bulk pH. The increase in the degree of dissociation of ionizable groups reduces the potential on the surface and inside the coating. However, as can be seen from the same diagram (cf. dashed curves), this reduction is less pronounced than would be the case for a potential-independent degree of dissociation, that is,

$$\alpha(z)=\mathrm{const}=\frac{1}{\frac{C_{H_3O^+}^{\infty}}{K_{\mathrm{a}}}+1}. \qquad (15)$$

Even if such an assumption is physically less meaningful, comparison of the obtained profiles with the potential distributions obtained by assuming a potential-dependent dissociation of the ionizable groups elucidates to which extent the decrease in layer and surface potential is attenuated by the counteracting effect of less ionization at lower potentials.

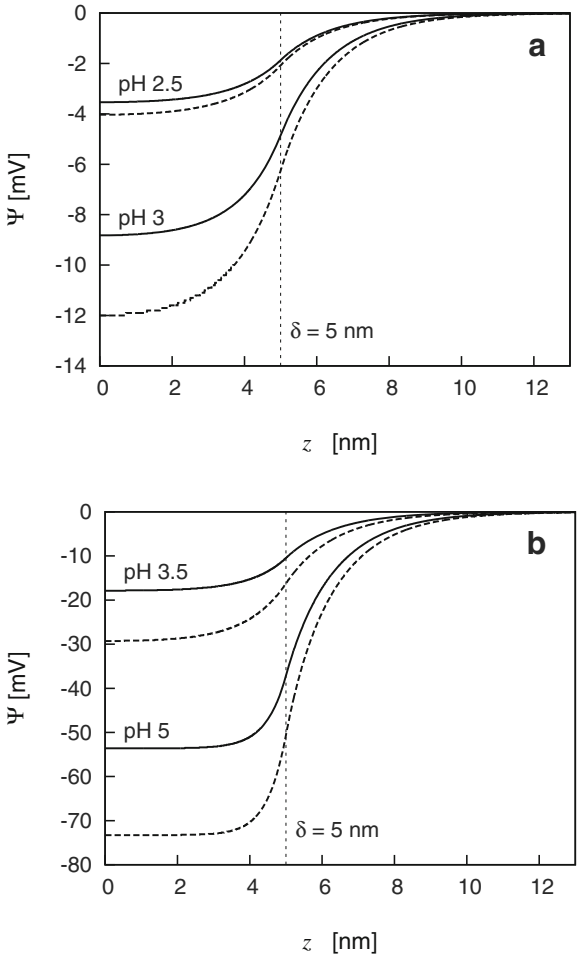

Figure 5 Effect of the bulk pH on the electric potential across the interface between the surface coating and the solution. Profiles obtained under the assumption of *z*-dependent ionization (——) are displayed together with the respective solutions for $\alpha(z)$ = const (- - - -) (see text). Calculation conditions are as follows: σ = 0; δ = 5 nm; $C_{H_3O^+}^{\infty} = 10^{-2.5}$ mol L^{-1} (**a**), 10^{-3} mol L^{-1} (**a**), $10^{-3.5}$ mol L^{-1} (**b**), 10^{-5} mol L^{-1} (**b**); C_{I}^{∞} = 0.05 mol L^{-1}.

Influence of the ionic strength on the potential distribution at noninteracting spore surfaces

Besides investigating the specific effects of the solution pH, we determined electric potential profiles of varying ionic strength for the case of a relatively low bulk pH value and a positive surface charge density.

As shown in Figure 6, the way in which the bulk ion concentration influences the surface potential in this case is a question of the thickness of the surface coating. When the coating is sufficiently thin so that the potential does not decay to negative values, the surface potential will generally rise with decreasing counterion concentration. This means that the highest surface potential will occur for the lowest ionic strength.

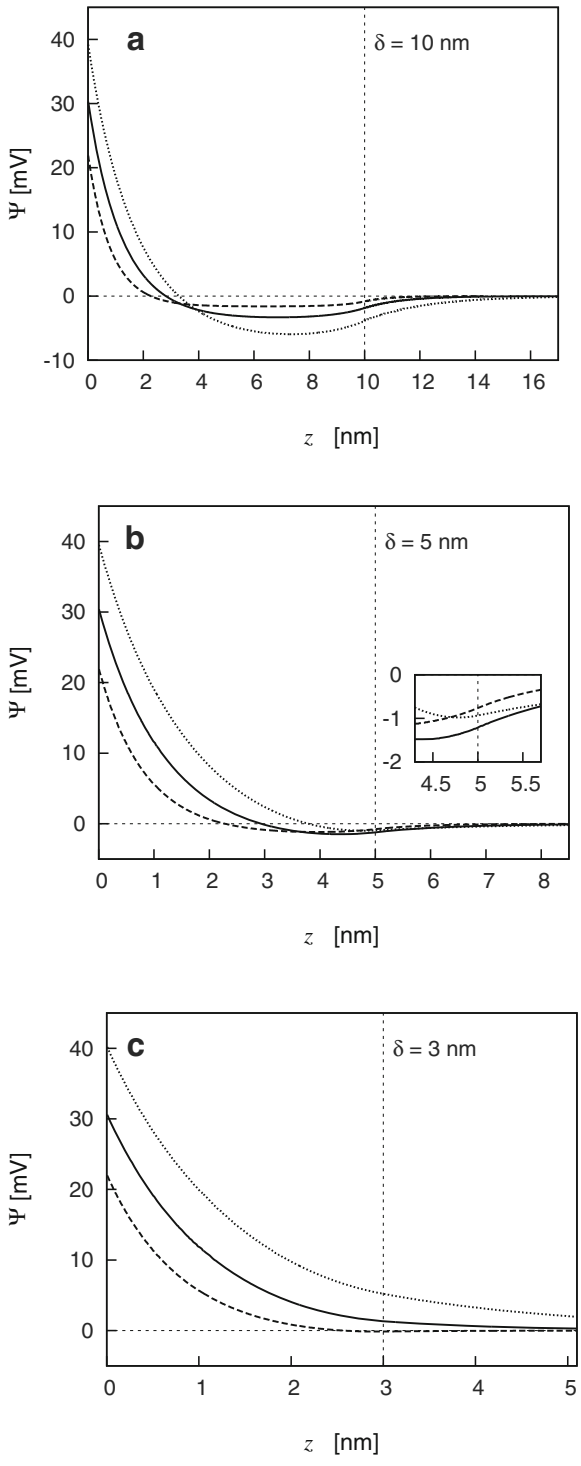

Figure 6 Influence of the bulk ion concentration on the electric potential profile at low bulk pH and different thicknesses of the surface coating. Calculating conditions are as follows: σ = 0.02 C m^{-2}; δ = 10 nm (**a**), 5 nm (**b**), 3 nm (**c**); $C^{\infty}_{H_3O^+} = 10^{-2.5}$ mol L^{-1}; C^{∞}_{I} = 0.02 mol L^{-1} (.....), 0.05 mol L^{-1} (____), 0.12 mol L^{-1} (-----).

Figure 6c depicts the results of an example calculation with δ = 3 nm, σ = 0.02 C m^{-2}, and $C^{\infty}_{H_3O^+} = 10^{-2.5}$ mol L^{-1}. Under these circumstances the surface potential is positive for C^{∞}_{I} values of 0.02 and 0.05 mol L^{-1}, whereas it is approximately zero for a C^{∞}_{I} of value 0.12 mol L^{-1}. According to expectations, the surface potential is greatest for C^{∞}_{I} = 0.02 mol L^{-1}. However, the opposite is true for the same conditions except that δ = 10 nm (Figure 6a). Here, the surface potential is smallest for C^{∞}_{I} = 0.02 mol L^{-1} and highest for C^{∞}_{I} = 0.12 mol L^{-1}. This particular behavior can be explained by considering once more electroneutrality in a thick coating. Under the assumption of a Boltzmann distribution of mobile ion concentrations, a reduction in the bulk ion concentration reduces the potential at which the total mean charge of the positive mobile ions counteracts the mean charge of all the negative ions. The profiles given in Figure 6b can be interpreted as an intermediate case. In this example, where δ = 5 nm, potentials are found to be quite similar in the region near the surface but still show interesting dependence on the bulk ion concentration. As can be seen from the inset of this diagram, the smallest surface potential is obtained for C^{∞}_{I} = 0.05 mol L^{-1}.

In addition to the above-discussed unspecific effect of the electrolyte ions, the solubility properties of the ions in the surface coating may also affect the surface potential. Figure 7 shows potential distributions for the calculation of which, ion solubilities of both positive and negative

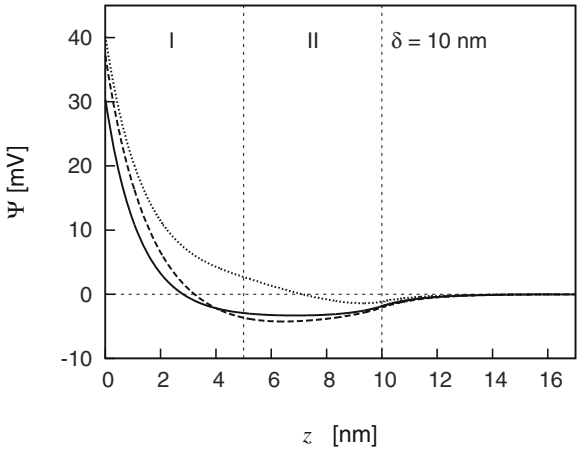

Figure 7 Impact of diminished ion solubilities on the electric potential distribution at low bulk pH. Profiles obtained for the cases where negative and positive mobile ions (-----) or negative mobile ions only (.....) possess lower solubilities in the coating are given in comparison with the respective solution for the case of uniform ion solubilities (____). Diminished solubilities were exemplarily considered by intrinsic partition coefficients that were 0.5 in region I and increased linearly from 0.5 to 1 across region II. Calculation conditions are as follows: σ = 0.02 C m^{-2}; δ = 10 nm; $C^{\infty}_{H_3O^+} = 10^{-2.5}$ mol L^{-1}; C^{∞}_{I} = 0.05 mol L^{-1}.

mobile ions or only negative mobile ions were assumed to be diminished. More precisely, the corresponding intrinsic partition coefficients were specified to be of value 0.5 within the inner half and to increase linearly from 0.5 to 1 within the outer half of the surface coating. The value of δ was chosen to be 10 nm and C_{I}^{∞} was set to 0.05 mol L^{-1}, while σ and $C_{\mathrm{H_3O^+}}^{\infty}$ were chosen as above. Comparing the profiles obtained for the symmetric ($b_+(z) = b_-(z) \leq 1$) and asymmetric ($b_-(z) \leq 1$ and $b_+(z) = 1$) cases to that obtained for the case of undiminished solubilities ($b_+(z) = b_-(z) = 1$) makes it clear that under these conditions, a more significant change in the potential distribution and, hence, in the surface potential is to be expected when only negative mobile ions exhibit a diminished solubility. This can be ascribed to the additional effect of the positive mobile ions to retard the decay of the potential, which will be most pronounced when their solubility remains undiminished.

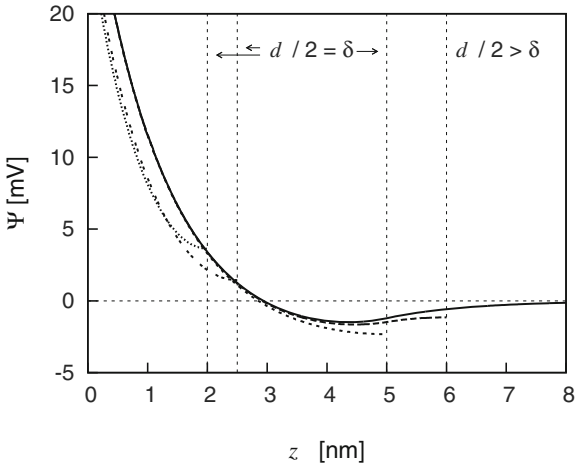

Figure 8 Dependence of the electric potential distribution on the distance between two interacting spore surfaces. Calculation conditions are as follows: σ = 0.02 C m^{-2}; δ^* = 5 nm; $C_{\mathrm{H_3O^+}}^{\infty} = 10^{-2.5}$ mol L^{-1}; C_{I}^{∞} = 0.05 mol L^{-1}; d = 24 nm (——), 12 nm (– – –), 10 nm (……), 5 nm (–.–.–), 4 nm (.....).

Potential distribution and electrostatic pressure between two spores

When two identically charged hard particles immersed in an electrolyte solution approach each other, the overlap of electric double layers will generally lead to an increase in the absolute value of the electric potential and also in the counterion concentration between them. As a consequence, the electrostatic stress acting on the particles' surfaces will no longer compensate for the excess osmotic pressure, resulting in a repulsive force. This force will steadily increase with decreasing distance and with decreasing ionic strength. In the case of two interacting spores, however, corresponding dependencies may be more complex, especially at pH values where we assume a positive charge contribution from the spore wall.

To consider the distance dependence of electrostatic spore–spore interaction at constant bulk ion concentration we focus on the midplane potential Ψ_{m}, that is, the electric potential at $z = d/2$. From equation 10, the electric field at this position is zero and hence so is the electrostatic stress. This implies that the electrostatic pressure between the spore surfaces is fully determined by the excess osmotic pressure at this position, and therefore, it is directly related to the midplane potential via [21]

$$P = 4N_{\mathrm{A}}C_{\mathrm{I}}^{\infty}kT\sinh^2\left(\frac{e\Psi_{\mathrm{m}}}{2kT}\right). \tag{16}$$

Figure 8 illustrates the change in the midplane potential with the distance between the surfaces, when σ = 0.02 C m^{-2}, δ^* = 5 nm, $C_{\mathrm{H_3O^+}}^{\infty} = 10^{-2.5}$ mol L^{-1}, and C_{I}^{∞} = 0.05 mol L^{-1}. The figure indicates that the midplane potential first decreases from zero to negative values as the spore surfaces are brought together but is then shifted in the opposite direction upon further reduction in d. Despite assuming an increased density of carboxyl groups for $\delta < \delta^*$, the midplane potential eventually changes its sign. Note that there is no electrostatic force acting on the surfaces at the distance at which the midplane potential crosses zero. In all other cases, the resulting electrostatic pressures will be repulsive

To elucidate the dependence of the repulsion on the bulk ion concentration at low pH, we determined the potential distributions and calculated the corresponding electrostatic pressures for the same conditions as above, except that C_{I}^{∞} was varied and d was kept constant at either 10 or 5 nm.

The resulting data plotted in Figure 9 reflect the complex dependence of electrostatic repulsion on the bulk ion concentration and the wall-to-wall distance between the interacting spore surfaces. In the case of uncompressed surface coatings in contact (d = 10 nm), the pressure passes through a maximum at a bulk ion concentration of about 0.1 mol L^{-1}. When choosing d = 5 nm, the same maximum occurs at an approximately three-fold higher value, while the pressure is minimal at around 0.1 mol L^{-1}.

As revealed by the corresponding potential distributions, the minimum originates from the crossing of the midplane potential through zero. The position of the obtained maxima, by contrast, cannot be deduced from the behavior of the midplane potential alone. This is because of the direct effect of the bulk ion concentration on the excess osmotic pressure when $\Psi_{\mathrm{m}} \neq 0$ (see equation 16). The reason for their occurrence can be understood, however, by noting that the midplane potential becomes minimal after changing its sign from positive to negative. This can be in turn explained in terms of the different

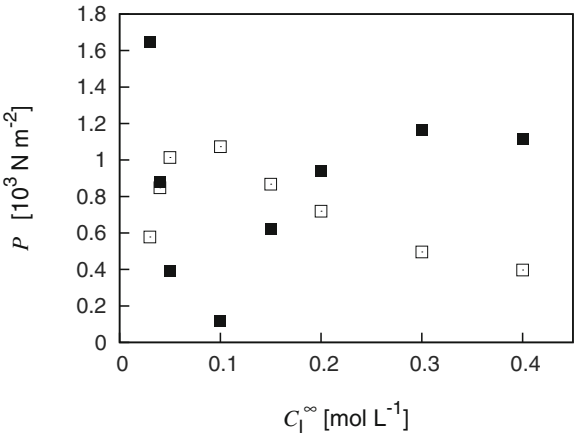

Figure 9 Electrostatic pressure between two spore surfaces as a function of the ion concentration in the bulk solution. Each point refers to a solution of the given Poisson–Boltzmann model for its specified ion concentration and other conditions as follows: σ = 0.02 C m^{-2}; δ^* = 5 nm; $C^{\infty}_{H_3O^+} = 10^{-2.5}$ mol L^{-1}; d = 5 nm (■), 10 nm (□).

dependence of the midplane potential on the bulk ion concentration for $\Psi_m \gg \Psi_l$ and $\Psi_m \approx \Psi_l$. Whereas in the former case, at lower concentrations, the midplane potential is dominated by the decay of the potential and will thus decrease with increasing concentration, the opposite is true at concentrations at which the midplane potential behaves like the layer potential.

Discussion

Most microbial cells feature a pH-dependent electric surface charge when immersed in aqueous solutions. This phenomenon can be attributed to the ionization of surface-associated basic and/or acidic functional groups. As the positive contribution of basic groups is more pronounced at lower pH and as negative charges from acidic groups dominate at higher pH, a cell that contains both basic and acidic groups at its surface is expected to exhibit a positive surface potential at lower pH values and a negative surface potential at higher pH values [27,28]. Some fungal spores, however, show electrokinetic behavior that indicates negative surface potentials down to pH values of 3 and smaller [11,29]. The same applies to the conidia of *A. niger*, which even appear to possess negative surface potentials down to a pH of 2 [10,12,20]. In our previous study [19], we traced this particular behavior to the presence of a melanin-containing surface coating on top of the outer spore wall. It was found that the zeta potential of the spores at pH 2 was shifted from a negative to positive values when the amount of melanin pigments was reduced by the preceding pigment extraction at higher pH values. From the results of an electrokinetic investigation of a melanin-deficient mutant [4] and chemical analysis of the extracted material, it was concluded that the surface potential of *A. niger* spores at low pH values is mainly determined by a net positively charged outer spore wall and a surface coating containing only acidic groups.

In the present study, the electrostatic interplay between the outer spore wall and the surface coating under acidic conditions was examined quantitatively via a Poisson–Boltzmann model. The negative charge within the coating was assumed to arise from carboxyl groups with a pK_a value of 4.3 [19]. A possible contribution from melanin-associated hydroxyl groups was neglected owing to the relatively high pK_a value of such weak acids. With this approach, we were able to model the expected shift in the surface potential from negative to positive values at low pH by reducing the thickness of the surface coating at a constant density of the carboxyl groups.

For comparing theoretically obtained surface potentials with the zeta potentials determined from electrophoretic data, one has to consider, in particular, the specific features of soft surfaces. In the case of cells carrying an ion-penetrable charged surface layer, the possible relative motion of the solution within the layer may account for an electrophoretic behavior that differs significantly from that of hard particles [17]. Hence, the simplification that electrophoretic mobility solely results from fluid movement beyond the surface, as assumed by the Smoluchowski equation, will not necessarily provide a good approximation. Surface potentials obtained for solutions of pH 2.5, pH 3, and pH 3.5 at a bulk ion concentration of 0.05 mol L^{-1} are nonetheless quite comparable to their respective zeta potentials. Experimental data are only 2.2 to 3.5 mV smaller. Moreover, under the assumption of a finite fluid drag inside the coating, a negative deviation of the zeta potential as calculated from the Smoluchowski equation would even be expected theoretically for a given distribution similar to those depicted in Figure 5 [30]. The zeta potential determined at pH 5 is, however, 18.8 mV greater than the corresponding surface potential. This notable difference cannot be ascribed to the simplified interpretation of experimentally determined mobilities. A possible explanation may lie in the extraction of melanin, which is much more pronounced at pH 5 than at the lower pH values [19]. If it is supposed that pigment release not only reduces the thickness of the coating as presumed above but also leads to a certain thinning of the coating, then the associated loss of charge would clearly entail an increase in the surface potential.

Regardless of the actual values of the surface potential at pH 5, it may be assumed from aggregation data that electrostatic interactions account for the absence of spore aggregation at this pH. The tendency of decreasing amount of spores present in aggregates with increasing pH is fully in line with expectations from electrokinetic data. By contrast, Grimm et al. [12] and Seviour

and Read [10], who both investigated aggregation of *A. niger* spores in culture media, were unable to link the observed pH dependence to electrostatic repulsion. In fact, they observed the opposite aggregation behavior. This difference is particularly remarkable in view of the results by Jones et al. [11], who found that incubation of *A. niger* spores in culture medium of pH 6.5 even caused a significant decrease of their respective electrophoretic mobilities in weakly acidic buffers. On the basis of this finding, it seems reasonable that reversible alterations in the electrostatic properties of the spores—and not biological alterations—are responsible for the apparently contradictory aggregation tendencies observed in certain media. Such alterations could arise from the specific adsorption of ions. Fungal melanins are well known for their ability to bind specific metal ions such as copper, calcium, magnesium, or zinc ions [31], which are typically present to a greater or lesser extent in culture media. Accordingly, it is quite conceivable that under certain cultivation conditions, specific cation adsorption shifts the net charge of the surface coating in the positive direction and, hence, the pH of minimum electrostatic repulsion toward higher values.

As there appears to be no marked affinity of sodium ions for melanin [32-34], we focused our theoretical investigations on the effect of electrolyte concentration on the diffusive behavior of the mobile ions. In fact, our model, which does not account for adsorption effects, is also able to provide an explanation for the dependence of the zeta potential on the NaCl concentration. This is easiest to understand by considering the cases for $\sigma \lesssim 0$ and $\sigma > 0$. In the former, the potential will be negative throughout the whole coating and, consequently, the potential near the surface will qualitatively depend on the bulk ion concentration as in the example shown in Figure 6a. Accordingly, it is expected to decrease with decreasing bulk ion concentration. This was obviously also true for zeta potentials obtained at pH 5 for instance. Since electrophoretic measurements of an albino mutant with similar background resulted in negative zeta potentials at this pH [4], it is most likely that the effective surface charge density at the boundary to the outer wall layer is actually negative. At pH 2.5, where albino spores exhibited a positive zeta potential, however, the electrophoretic mobility of the melanized spores first decreased but then increased again when the NaCl concentration was further reduced from 0.05 to 0.01 mol L^{-1}. A possible explanation within the framework of our model is the influence of the thickness of the surface coating on the dependence of the bulk ion concentration on the surface potential for $\sigma > 0$. If we presume that the thickness of the surface coating varies from spore to spore and that a number of spores possess positive surface potentials at a certain low electrolyte concentration, the tendency of decreasing average mobility with decreasing electrolyte concentration will undoubtedly be attenuated or even reversed by the mobility increase of the spores possessing the positive surface potentials. Nonetheless, it should be noted here that, as demonstrated in Figure 6b, a minimum can even occur in the theoretical case where all spores exhibit more or less the same surface properties. Although it appears unlikely with respect to our previous investigations [19] that the large majority of the spores possess a surface coating approximately 5 nm thick, such a situation is quite conceivable for the case in which ion solubilities in the surface coating are assumed to be diminished. Especially for the hypothetical case where chloride ions only show a diminished solubility, the associated reduction in the decay of the potential would shift the range of thicknesses at which the surface coating features such intermediate character to greater values.

Even though the observed pH-dependent aggregation tendency is found to be in good agreement with the conventional predictions based on the zeta potential, the dependence of spore aggregation on the NaCl concentration at a pH of 2.5 is difficult to deduce from direct comparison with zeta potentials. Within the framework of the classical colloidal theories for hard particles, it is predicted that both the zeta potential and the aggregation rate show a monotonic dependence on the salt concentration. More precisely, the absolute value of the zeta potential is expected to decrease with the increasing salt concentrations, while the aggregation rate is expected to increase. The dependence of the aggregation rate on the salt concentration is explained using the DLVO theory. According to this theory, the electrostatic energy barrier between two like-charged particles is more pronounced when the bulk ion concentration is lower and the thickness of the diffuse double layer is greater. If electrostatic attraction effects are prevalent, on the other hand, aggregation can also be accelerated with decreasing ionic strength. Prominent examples of such behavior include the attachment of oppositely charged polyelectrolytes to the surfaces of like-charged particles [35,36]; in this particular case, it is believed that the electrostatic attractions arise from the resulting lateral surface charge inhomogeneities.

It is quite conceivable that similar inhomogeneities also affect the aggregation behavior of the spores. However, we hypothesize that the observation of an aggregation maximum can best be explained by considering the actual charge distribution along the surface normal. This notion is supported by the theoretical results presented in Figure 9. These results clearly indicate that with a constant distance between the spores, the repulsion reaches a maximum, and under certain circumstances, also a minimum with a reduction in the bulk ion concentration. The

occurrence of a pressure minimum at a bulk ion concentration of order 0.1 mol L^{-1} in turn may be related to the observed aggregation maximum. Based on our theoretical assumptions this would most likely be the case when the surface coatings are compressed. To comprehend why a reduced repulsion under these sterically unfavored conditions can potentially entail an aggregation maximum, one should keep in mind that the equilibrium distance between two interacting spores will be a question of the entirety of reversible interactions. These interactions additionally involve attractive van der Waals and, probably, also attractive hydrophobic interactions [6]. The addition of these position-dependent interactions gives a theoretical equilibrium distance at which the binding between the spores is most stable. By taking into account that for a certain constant bulk ion concentration, the midplane potential between two approaching spores crosses zero at a certain distance, it is plausible that one can associate a bulk ion concentration with each equilibrium distance such that there will be no additional electrostatic repulsion. At smaller or greater bulk ion concentrations, the binding would then most likely be less stable, and thus, an aggregation maximum is to be expected at exactly this bulk ion concentration.

Conclusions

In order to comprehend the effect of pH and ionic strength on the aggregation behavior of *A. niger* spores, we investigated their electrostatic surface properties in simple electrolyte solutions and compared these properties with the results of aggregation experiments.

We found a strong dependence of the aggregation behavior on the pH value. At pH 5, where we expect a relatively high negative surface potential due to an increased ionization of melanin bound carboxyl groups, very little to no aggregation occurred. The highest aggregation, on the other hand, was observed for pH 2.5. At this pH we expect the spores to possess a surface potential around zero.

It is remarkable to note that spore aggregation, nonetheless, showed a clear dependence on the electrolyte concentration at pH 2.5, indicating electrostatic interactions to still be relevant. With the increase in electrolyte concentration, the tendency to form aggregates first increased and then decreased. While such behavior can hardly be explained by theories that assume the surface charge to be located in a single plane, our model, which accounts for the effects of a nonuniform charge distribution within a certain depth below the actual surface, predicts the occurrence of an aggregation maximum.

Thus, this work not only demonstrates the relevance of electrostatic interactions for *A. niger* spore aggregation, but also exemplifies the importance of knowledge on the origin and spatial distribution of the surface charge in cell–cell interactions. In particular, for melanized cells, we suggest that a differentiated consideration of charge contributions is a prerequisite for understanding the influence of electrostatic interactions on microbial cell aggregation.

Additional file

Additional file 1: Description of data: Numerical approach for solving the Poisson-Boltzmann model equations.

Competing interests

The authors declare that they have no competing interests.

Authors' contributions

Aggregation experiments, electrophoretic measurements, and the modeling were carried out by AW. IK participated in the design of the aggregation experiments and contributed to the data analysis. The study was coordinated by AK, who also helped draft the manuscript. All authors read and approved the final manuscript.

Acknowledgements

The authors gratefully acknowledge the financial support provided by the German Research Center (DFG) through the collaborative research center SFB 578.

Received: 7 December 2012 Accepted: 25 January 2013
Published: 28 February 2013

References

1. Gerin P, Bellon-Fontaine MN, Asther M, Rouxhet PG (1995) Immobilization of fungal spores by adhesion. Biotechnol Bioeng 47: 677–687
2. Webb JS, van der Mei HC, Nixon M, Eastwood IM, Greenhalgh M, Read SJ, Robson GD, Handley PS (1999) Plasticizers increase adhesion of the deteriogenic fungus *Aureobasidium pullulans* to polyvinyl chloride. Appl Environ Microbiol 65: 3575–3581
3. Bowen WR, Lovitt RW, Wright CJ (2000) Direct quantification of *Aspergillus niger* spore adhesion in liquid using an atomic force microscope. J Colloid Interface Sci 228: 428–433
4. Priegnitz BE, Wargenau A, Brandt U, Rohde M, Dietrich S, Kwade A, Krull R, Fleißner A (2012) The role of initial spore adhesion in pellet and biofilm formation in *Aspergillus niger*. Fungal Genet Biol 49: 30–38
5. Dynesen J, Nielsen J (2003) Surface hydrophobicity of *Aspergillus nidulans* conidiospores and its role in pellet formation. Biotechnol Prog 19: 1049–1052
6. Wargenau A, Kwade A (2010) Determination of adhesion between single *Aspergillus niger* spores in aqueous solutions using an atomic force microscope. Langmuir 26: 11071–11076
7. Harding MW, Marques LLR, Howard RJ, Olson ME (2009) Can filamentous fungi form biofilms? Trends Microbiol 17: 475–480
8. Grimm LH, Kelly S, Krull R, Hempel DC (2005) Morphology and productivity of filamentous fungi. Appl Microbiol Biotechnol 69: 375–384
9. Metz B, Kossen NWF (1977) The growth of molds in the form of pellets – a literature review. Biotechnol Bioeng 19: 781–799
10. Seviour RJ, Read MA (1985) Electrophoretic mobility of conidia of *Aspergillus niger*, and the role of their surface properties in pelleting. Trans Br Mycol Soc 84: 745–747
11. Jones P, Moore D, Trinci APJ (1988) Effects of Junlon and Hostacerin on the electrokinetic properties of spores of *Aspergillus niger*, *Phanerochaete chrysosporium* and *Geotrichum candidum*. J Gen Microbiol 134: 235–240
12. Grimm LH, Kelly S, Völkerding II, Krull R, Hempel DC (2005) Influence of mechanical stress and surface interaction on the aggregation of *Aspergillus niger* conidia. Biotechnol Bioeng 92: 879–888
13. Donath E, Pastushenko V (1979) Electrophoretical study of cell surface properties. The influence of the surface coat on the electric potential distribution and on general electrokinetic properties of animal cells. Bioelectrochem Bioenerg 6: 543–554

14. Heinrich R, Gaestel M, Glaser R (1982) The electric potential profile across the erythrocyte membrane. J Theor Biol 96: 211–231
15. Ohshima H, Ohki S (1985) Donnan potential and surface potential of a charged membrane. Biophys J 47: 673–678
16. Inoue S, Ohshima H, Kondo T (1989) Boundary potential and membrane potential of *Physarum polycephalum:* effects of electrolyte ions and chloroform. J Colloid Interface Sci 130: 211–218
17. Ohshima H (2007) Electrokinetics of soft particles. Colloid Polym Sci 285: 1411–1421
18. Ohshima H (2008) Electrostatic interaction between soft particles. J Colloid Interface Sci 328: 3–9
19. Wargenau A, Fleißner A, Bolten CJ, Rohde M, Kampen I, Kwade A (2011) On the origin of the electrostatic surface potential of *Aspergillus niger* spores in acidic environments. Res Microbiol 162: 1011–1017
20. Hannan PJ (1961) Electrophoretic properties of spores of *Aspergillus niger*. Appl Microbiol 9: 113–117
21. Ohshima H (2006) Theory of colloid and interfacial electric phenomena. Academic Press, London
22. Makino K, Ohshima H, Kondo T (1987) Potential distribution across membranes with surface-charge layers. Effects of ionic solubility. Colloid Polym Sci 265: 336–341
23. Mattern IE, van Noort JM, van den Berg P, Archer DB, Roberts IN, van den Hondel CAMJJ (1992) Isolation and characterization of mutants of *Aspergillus niger* deficient in extracellular proteases. Mol Gen Genet 234: 332–336
24. Lin PJ, Scholz A, Krull R (2010) Effect of volumetric power input by aeration and agitation on pellet morphology and product formation of *Aspergillus niger*. Biochem Eng J 49: 213–220
25. Lyklema J (2003) Electrokinetics after Smoluchowski. Colloids Surf, A 222: 5–14
26. Zlokarnik M, Judat H (1988) Stirring. In: Unit Operations I. (Ed) Gerhartz W. VCH , Weinheim, pp 25.1–25.33. [Arpe HJ , Biekert E , Davis HT , Gerrens H , Kametani T , McGuire JL , Mitsutani A , Pilat H , Reece C , Sheetz DP , Simmons HE , Weise E , Wirtz R , Wüthrich HR (Series Editors), Ullmann's Encyclopedia of Industrial Chemistry, vol B2.]
27. Prieve DC, Ruckenstein E (1976) The surface potential of and double-layer interaction force between surfaces characterized by multiple ionizable groups. J Theor Biol 56: 205–228
28. Shinagawa T, Ohshima H, Kondo T (1992) Isoelectric point of an ion-penetrable membrane. Biophys Chem 43: 149–156
29. Fisher DJ (1973) Charges on fungal spores. Pestic Sci 4: 845–860
30. Ohshima H (1994) Electrophoretic mobility of soft particles. J Colloid Interface Sci 163: 474–483
31. Fogarty RV, Tobin JM (1996) Fungal melanins and their interactions with metals. Enzyme Microb Technol 19: 311–317
32. Gadd GM, de Rome L (1988) Biosorption of copper by fungal melanin. Appl Microbiol Biotechnol 29: 610–617
33. Potts AM, Au PC (1976) The affinity of melanin for inorganic ions. Exp Eye Res 22: 487–491
34. Felix CC, Hyde JS, Sarna T, Sealy RC (1978) Interactions of melanin with metal ions. Electron spin resonance evidence for chelate complexes of metal ions with free radicals. J Am Chem Soc 100: 3922–3926
35. Bouyer F, Robben A, Yu WL, Borkovec M (2001) Aggregation of colloidal particles in the presence of oppositely charged polyelectrolytes: effect of surface charge heterogeneities. Langmuir 17: 5225–5231
36. Popa I, Gillies G, Papastavrou G, Borkovec M (2009) Attractive electrostatic forces between identical colloidal particles induced by adsorbed polyelectrolytes. J Phys Chem B 113: 8458–8461

doi:10.1186/1559-4106-8-7
Cite this article as: Wargenau *et al.*: **Linking aggregation of *Aspergillus niger* spores to surface electrostatics: a theoretical approach.** *Biointerphases* 2013 **8**:7.